

A.F. Moene^{1*} and A. van Dijk^{1,2}¹ Meteorology and Air Quality Group, Wageningen University, The Netherlands² Alterra, Wageningen University and Research Center, The Netherlands

1. Introduction

Turbulent spectra of scalars exhibit a peculiar behaviour in the near-dissipation range, i.e. at length scales of the order of the Taylor length scale. Around this length scale the velocity fluctuations make a transition from inertial motion to viscous dissipation. At about the same scale, depending on either the Prandtl number (Pr , temperature) or Schmidt number (Sc , mass), the scalar fluctuations transit from convective motion to diffusion. The shape of the scalar spectrum depends on the relative location of that transition in the velocity spectrum and the scalar spectrum. For Pr or $Sc \ll 1$, there is an inertial-convective range, a viscous-convective range and a viscous-diffusive range. On the other hand, if Pr or $Sc \gg 1$ there is an inertial-convective range, an inertial-diffusive range and a viscous-diffusive range.

In scintillometry, the exact shape of particularly the temperature and humidity spectra is very important. Laser scintillometers (both single and double beam scintillometers) are sensitive to temperature (and humidity) fluctuations in the transition range from inertial range to dissipation range (see e.g. Hartogensis et al. (2002)). Furthermore, large aperture scintillometers become sensitive to fluctuations at those small scales when the signal becomes saturated (Kohsiek et al., 2006).

Up to now, the analysis of scintillometer signals in which the dissipation range is relevant, the model spectrum of Hill (1978) is used.

In this note an alternative estimation of the scalar spectrum is presented. This estimation builds on the results obtained by Tatarskii (2005) for the velocity spectrum. Like Hill's model, the spectrum resulting from our method exhibits a similar bump as Hill's model. Our result is compared to the same experimental data as done in Hill (1978).

2. Derivation of scalar spectra

A general definition of the structure function for one or two variables for homogeneous, isotropic turbulence is:

$$D_{a^\alpha b^\beta}(r) \equiv \overline{(a(x+r) - a(x))^\alpha (b(x+r) - b(x))^\beta} \quad (1)$$

where a and b are two quantities and α and β are integral exponents and r is the separation. In this paper a and b are the longitudinal velocity u (i.e. velocity component parallel to r) and a scalar concentration. Here temperature T is used for the scalar and consequently Pr for the

ratio of viscosity and the scalar diffusivity (here χ). But T could be replaced by any other scalar, while replacing Pr by the Schmidt number Sc and χ by the appropriate diffusivity.

Based on the Navier-Stokes equation, and the transport equation for heat, differential equations for D_{uu} and D_{TT} can be derived (under conditions of incompressibility, local stationarity, local isotropy and local homogeneity):

$$D_{uuu}(r) - 6\nu \frac{d}{dr} D_{uu}(r) = -\frac{4}{5} \bar{\epsilon} r \quad (2)$$

$$D_{TTu}(r) - 2\chi \frac{d}{dr} D_{TT}(r) = -\frac{4}{3} \bar{N}_T r \quad (3)$$

where D_{TTu} is a third-order mixed structure function, ν is the kinematic viscosity, χ is the thermal molecular diffusivity, $\bar{\epsilon}$ is the dissipation of turbulent kinetic energy, and \bar{N}_T is the dissipation of temperature variance. Details on the conditions under which the derivation of equation 2 is valid can be found in Hill (1997).

Using dimensional analysis, the following similarity relationships for the structure functions mentioned above can be deduced:

$$D_{uu}(r) = (\bar{\epsilon}\nu)^{1/2} f_{uu}(\xi) \quad (4)$$

$$D_{TT}(r) = \frac{\bar{N}_T}{\epsilon} (\bar{\epsilon}\nu)^{1/2} f_{TT}(\xi) \quad (5)$$

$$D_{TTu}(r) = \frac{\bar{N}_T}{\epsilon} (\bar{\epsilon}\nu)^{3/4} f_{TTu}(\xi), \quad (6)$$

where $\xi = r/\eta$, and η is the Kolmogorov length scale $(\nu^3/\bar{\epsilon})^{1/4}$. f_{TT} , f_{uu} and f_{TTu} are similarity functions that need to be determined either from limiting cases, or from experiments. For two limiting cases, the r -dependence of f_{uu} , f_{TT} and f_{TTu} can be predicted. For the inertial-convective subrange, the viscosity and thermal diffusivity become irrelevant, f_{uu} and f_{TT} both become proportional to $r^{2/3}$ and $f_{TTu} \sim r$. In the dissipation range, f_{uu} and f_{TT} are quadratic in r and f_{TTu} is assumed to be cubic (Kolmogorov, 1941).

The differential equations 2 and 3 can be rewritten as:

$$\frac{1}{6} f_{uuu}(r) - \frac{d}{d\xi} f_{uu}(r) = -\frac{2}{15} \xi \quad (7)$$

$$\frac{Pr}{2} f_{TTu}(\xi) - \frac{d}{d\xi} f_{TT}(\xi) = -\frac{2}{3} Pr \xi. \quad (8)$$

In order to solve for f_{TT} (i.e. D_{TT}), an estimate for f_{TTu} is needed. To this end, use is made of the mixed skewness $F(r)$, defined as:

$$F(r) \equiv \frac{D_{TTu}(r)}{\sqrt{D_{uu}(r)D_{TT}(r)}} = \frac{f_{TTu}(r)}{\sqrt{f_{uu}(r)f_{TT}(r)}} \quad (9)$$

* Corresponding author address: Arnold F. Moene, Meteorology and Air Quality Group, Wageningen University, Duivendaal 2, 6701 AP Wageningen; e-mail: arnold.moene@wur.nl

Substitution of equation 9 into 8 yields:

$$\frac{Pr}{2} F(r) \sqrt{f_{uu}(\xi)} f_{TT}(\xi) - \frac{d}{d\xi} f_{TT}(\xi) = -\frac{2}{3} Pr \xi. \quad (10)$$

In a similar way, f_{uuu} in 7 can be replaced by a combination of the skewness $S(r)$ and f_{uu} . Except for quantification of $F(r)$ and $S(r)$, D_{TT} can now be solved for.

A commonly used assumption is that $F(r)$ is independent of the separation (which at least it is in the two limiting cases of inertial subrange and dissipation range, see above). Then, if $F(r)$ is known from the limiting cases, as well as the similarity function for the velocity structure function (f_{uu}), the differential equation for f_{TT} can be solved. The solution of equation 2 was dealt with by Tatarskii (2005), yielding the required f_{uu} . Apart from the assumption of constant $F(r)$ (and $S(r)$), we will investigate the consequences of $F(r)$ and $S(r)$ varying with r as well.

In the end one is interested in the shape of the scalar spectrum (be it the three-dimensional spectrum $\Gamma(k)$ or the one-dimensional spectrum $\Psi(k_1)$). To arrive at the spectra for the scalar, the following transformation is used:

$$\Gamma_{TT}(k) = \frac{1}{2\pi k} \int_0^\infty \sin(k\xi) \frac{dD_{TT}}{d\xi} d\xi. \quad (11)$$

To go from $\Gamma(k)$ to $\Psi(k_1)$ the following relationship can be used (Hill, 1978):

$$\Psi(k_1) = \int_{k_1}^\infty \frac{\Gamma(k)}{k} dk. \quad (12)$$

3. Comparison to data

In this section scalar spectra according to the methodology presented in the previous section will be derived. First constant (independent of r) values for the skewnesses $S(r)$ and $F(r)$ will be assumed (section 3.1). Next a variable skewness will be used, based on the DNS results of Watanabe and Gotoh (2004) (section 3.2).

The resulting spectra for the longitudinal windspeed will be compared to experimental results of Saddoughi (1997) and Williams and Paulson (1977). The temperature spectra are compared to data from Williams and Paulson (1977) and Champagne et al. (1977). Furthermore, the DNS results of Watanabe and Gotoh (2004) are included for comparison as well (with $Pr = 0.7$).

3.1 Constant mixed skewness

Like Obukhov and Yaglom (1951) the skewness $S(r)$ is assumed to be independent of wavenumber. Furthermore, the same assumption will be made for the mixed skewness $F(r)$. However, there is significant uncertainty regarding the value of $S(r)$ (see Katul et al. (1995) and Katul et al. (1997) for a discussion). The values range between -0.25 and -0.5. Katul et al. (1995) show that the value of -0.25 is consistent with a Kolomogorov constant equal to 0.55. For $S(r)$ a reference value of -0.25 is used. For $F(r)$ -0.4 is used. The results for the velocity

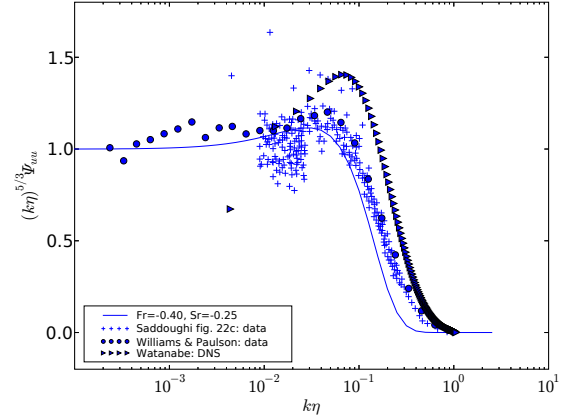


FIG. 1: Compensated longitudinal velocity spectrum derived from 7, with constant $S(r) = -0.25$. The result is compared with experimental data of Saddoughi (1997) and Williams and Paulson (1977) and DNS results of Watanabe and Gotoh (2004).

spectrum can be found in figure 1. The model is quite close to the data of Saddoughi (1997), whereas the DNS results show a much too high bump. This may in part be due to an incorrect estimation of the inertial subrange level of the spectrum (in the graph the spectra have been normalized with the mean value for $k\eta < 0.025$).

3.2 Wavenumber-dependent mixed skewness

Katul et al. (1995) investigated for a limited number of cases the constancy of $S(r)$ with separation. Given their experimental facilities, they only could resolve separations within the inertial subrange (or larger). For that range of separations they conclude that $S(r)$ is relatively constant at a value somewhat larger than the accepted value of -0.4. In order to find any r -dependence of $S(r)$ and $F(r)$ at separations below the inertial subrange experimental data at very small scales would be needed. For the velocity skewness $S(r)$ this might be feasible, but for the mixed skewness $F(r)$ simultaneous velocity and temperature data would be needed. Since we do not have those data at our disposal, we revert to DNS results obtained by Gotoh and Watanabe (personal communication). The simulation used is similar to those reported in Watanabe and Gotoh (2004), except that $Pr = 1$ and the turbulent Reynolds number $R_\lambda = 427$. The resulting separation dependence of $S(r)$ and $F(r)$ is shown in figure 5. It appears that for $40 < r/\eta < 150$ both skewnesses are rather constant. For larger separations the size of the computational domain influences the results. A test on resolution dependence of the structure parameter, performed by Gotoh and Watanabe (personal communication) showed that for $r/\eta > 10$ the results were resolution independent. Thus, the decrease in $S(r)$ and $F(r)$ from their inertial subrange values can be trusted down to about $r/\eta > 10$.

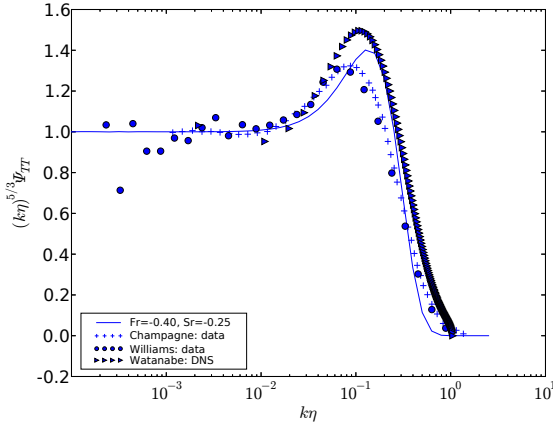


FIG. 2: Compensated temperature spectrum derived from 10, with $S(r) = -0.25$ and $F(r) = -0.4$ and $Pr = 0.72$. The result is compared with experimental data of Williams and Paulson (1977) and Champagne et al. (1977) and DNS results of Watanabe and Gotoh (2004).

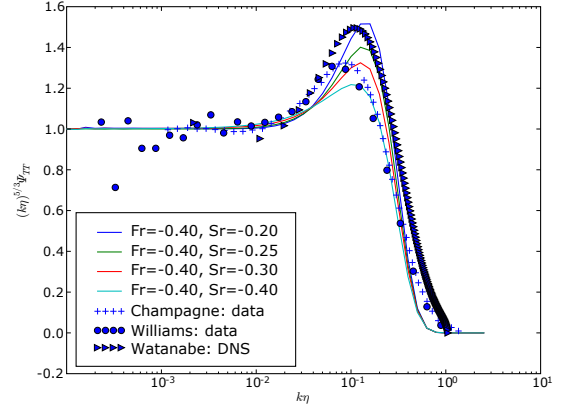


FIG. 4: Compensated temperature spectrum derived from 10, with a range of $S(r)$ values and a range of $F(r) = -0.40$ values and $Pr = 0.72$. The result is compared with experimental data of Williams and Paulson (1977) and Champagne et al. (1977) and DNS results of Watanabe and Gotoh (2004).

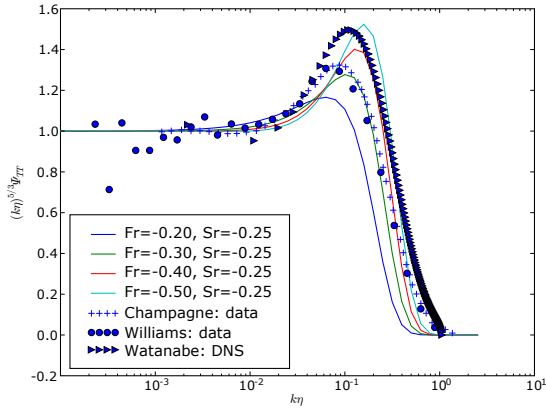


FIG. 3: Compensated temperature spectrum derived from 10, with $S(r) = -0.25$ and a range of $F(r)$ values and $Pr = 0.72$. The result is compared with experimental data of Williams and Paulson (1977) and Champagne et al. (1977) and DNS results of Watanabe and Gotoh (2004).

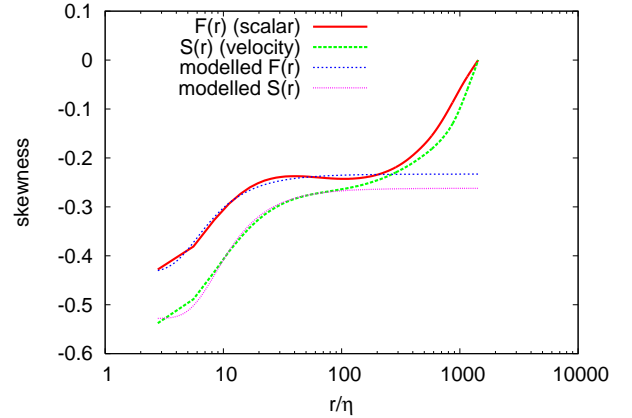


FIG. 5: Skewness $S(r)$ and $F(r)$ as derived from the DNS results of with $Pr = 1$ and $R_\lambda = 427$. Also included are the models according to 14.

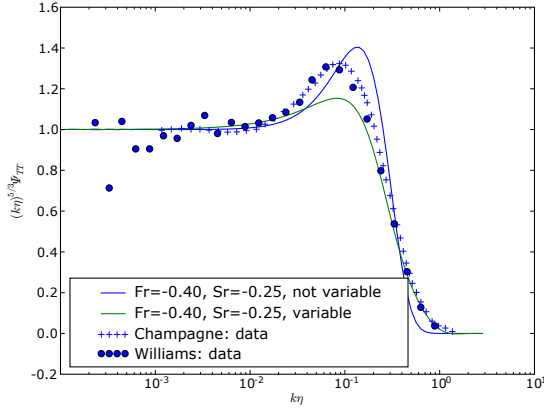


FIG. 6: Compensated temperature spectrum derived from 10, with constant values for $S(r)$ and $F(r)$, as well as $S(r)$ and $F(r)$ according to 14 with S_1 and S_2 set to -0.25 , F_1 and F_2 set to -0.40 and $Pr = 0.72$. The result is compared with experimental data of Williams and Paulson (1977) and Champagne et al. (1977).

From figure 5 it can be concluded that for $r/\eta < 40$ $S(r)$ and $F(r)$ decrease from values around -0.25 to approximately -0.5 . The r -dependence can reasonably well be described with:

$$F(r)_{model} = F_1 + F_2 \tanh\left(F_3/r^{3/2}\right) \quad (13)$$

$$S(r)_{model} = S_1 + S_2 \tanh\left(S_3/r^{3/2}\right) \quad (14)$$

with $F_1 = -0.233$, $F_2 = -0.2003$, $F_3 = 11.38$, $S_1 = -0.262$, $S_2 = -0.266$ and $S_3 = 19.54$. Note that the inertial subrange values for $F(r)$ differs considerably from the reference value of -0.40 used before.

Figure 6 shows the temperature spectra resulting from using equation 14 to parameterize the r -dependence of $S(r)$ and $F(r)$ (but with S_1 and S_2 set to -0.25 , F_1 and F_2 set to -0.40). The comparison to spectra calculated with constant $S(r)$ and $F(r)$ reveals that the non-constant $S(r)$ and $F(r)$ cause the height of the bump to decrease and to make the high-wavenumber fall-off less steep.

4. Conclusion and discussion

It was shown how the one-dimensional temperature spectrum can be derived from the conservation equations of the longitudinal (second order) structure function for velocity and the (second order) structure function of temperature. This model has two closure parameters, $S(r)$ and $F(r)$ which are the skewness of the velocity structure function and the mixed skewness of the temperature-velocity structure function. It is common to take $S(r)$ and $F(r)$ constant with r and fixed to the inertial subrange value. This has the advantage that the latter is easily obtained from field data. However, recent DNS results

suggest that for $r/\eta < 40$ the skewness decrease considerably (to lower negative values). It has been shown that incorporation of this variability of $S(r)$ and $F(r)$ has a significant impact on the temperature spectrum.

Further research is needed to validate the proposed model for the temperature spectrum. Especially the exact shape of $S(r)$ and $F(r)$ and its possible dependence on the Reynolds number needs to be explored. Furthermore, the consequences of the variability in the shape of the temperature spectrum on the interpretation of scintillometer signals needs to be explored. Finally, the variability of the inertial subrange values of $S(r)$ and $F(r)$ with atmospheric conditions (mainly stability) needs to be investigated.

Acknowledgements

We greatly acknowledge the cooperation of T. Gotoh and T. Watanabe for providing us with their published and unpublished DNS results.

REFERENCES

- Champagne, F.H., C.A. Friehe, J.C. LaRue, and J.C. Wyngaard, 1977: Flux measurements, flux estimation techniques, and fine-scale turbulence measurements in the unstable surface layer over land. *J. Atmos. Sci.*, **34**, 515–530.
- Hartogensis, O.K., H.A.R. DeBruin, and B.J.H. van de Wiel, 2002: Displaced-beam small aperture scintillometer test. Part II: CASES-99 stable boundary layer experiment. *Boundary-Layer Meteorology*, **105**, 149–176.
- Hill, R.J., 1978: Models of the scalar spectrum for turbulent advection. *J. Fluid Mech.*, **88**, 541–562.
- Hill, R.J., 1997: Applicability of Kolmogorov's and Monin's equations of turbulence. *J. Fluid Mech.*, **353**, 67–81.
- Katul, G.G., C.I. Hsieh, and J. Sigmon, 1997: Energy-inertial scale interactions for velocity and temperature in the unstable atmospheric surface layer. *Boundary-Layer Meteorology*, **82**, 49–80.
- Katul, G.G., M.B. Parlange, J. Albertson, and C. Chu, 1995: Local isotropy and anisotropy in the sheared and heated atmospheric surface layer. *Boundary-Layer Meteorology*, **72**, 123–148.
- Kohsiek, W., W.M.L. Meijninger, H.A.R. De Bruin, and F. Beyrich, 2006: Saturation of the large aperture scintillometer. *Boundary-Layer Meteorology* doi:10.1007/s10546-005-9031-7.
- Kolmogorov, A.M., 1941: The local structure of turbulence in incompressible viscous fluid for very large Reynolds numbers. *C. R. Acad. Sci. URSS*, **30**, 301–305.

- Obukhov, A.M. and A.M. Yaglom, 1951: The microstructure of turbulent flow. *Prikl. Mat. Mekh.*, **15**, 3. In Russian. Translated into English in NACA Technical Memorandum 1350 (1953).
- Saddoughi, S.G., 1997: Local isotropy in complex turbulent boundary layers at high Reynolds number. *J. Fluid Mech.*, **348**, 201–245.
- Tatarskii, V.I., 2005: Use of the 4/5 Kolmogorov equation for describing some characteristics of fully developed turbulence. *Phys. Fluids*, **14**, 035110–1–12.
- Watanabe, T. and T. Gotoh, 2004: Statistics of a passive scalar in homogeneous turbulence. *New Journal of Physics*, **6**, 40.
- Williams, R.M. and C.A. Paulson, 1977: Microscale temperature and velocity spectra in the atmospheric boundary layer. *J. Fluid Mech.*, **83**(547–567).